Study on Creep Test and Constitutive Model of Layered Soft Rock

Chun Liu, Heng Liu*, Haizhuang Liu, Yiying Xiong, Chao Tang, Zexi Zhou

Safety Engineering College, Chongqing University of Science and Technology, Chongqing 401331, China

*E-mail: 786926856@qq.com

Abstract. The basic mechanical parameters of rock are obtained and the creep curves under different stress loads are obtained to reveal the creep law of layered soft rock under different stress loads. According to the creep test results, the linear Burgers creep model is used to fit the test data. The fitting effect of the attenuation creep stage and stable creep stage is better, and the fitting effect of the accelerated creep stage is poor. To describe the accelerated creep stage of layered rock more accurately, based on the Mohr-Coulomb strength criterion, a plastic element is introduced, which is connected in series with the linear Burgers creep model to form an improved nonlinear Burgers creep model. The model is used to re-fit the experimental data. The results show that the fitting effect of the accelerated creep stage is significantly better than that of the linear creep model. The nonlinear Burgers creep model file is compiled by using FISH language embedded in FLAC3D for numerical simulation analysis, and the creep results are compared with the field monitoring data. The change rule of the two data is close, indicating that the improved nonlinear model can more accurately describe the creep characteristics of layered soft rock.

Keywords: layered soft rock; creep test; creep constitutive model; data fitting; the numerical simulation

1 Introduction

At present, there are some achievements in the study of rock creep characteristics test and constitutive model at home and abroad[1-8]. A numerical method based on the particle discrete element method is studied to describe the typical creep behavior of phyllite, including its attenuation, stability, accelerated creep stage, and transverse isotropic, according to, designed by Zhang et al[9]. The creep model and parameter inversion of columnar jointed basalt are studied. Wei et al. proposed the generalized Kelvin model, and the compression creep formula of the intermediate measuring point of the flexible double pillow compression plate is derived [10]. The unloading creep tests of deep sandstone under different initial stresses and water pressures were carried out by

D. Li et al. (eds.), *Proceedings of the 2023 9th International Conference on Architectural, Civil and Hydraulic Engineering (ICACHE 2023)*, Advances in Engineering Research 228,
https://doi.org/10.2991/978-94-6463-336-8_8

using the TFD-2000 rock triaxial rheological test system. The deformation characteristics of rock mass in the attenuation and stable creep stages under different stresses and water pressures were analyzed.

Based on the results of the conventional compression test and creep test of layered soft rock, linear and improved nonlinear Burger's creep models are compared to describe the attenuation creep, stable creep, and accelerated creep stages of rock. The fitting of experimental data shows that the nonlinear visco-elastic-plastic model can more accurately reflect the characteristics of the rock creep stage, and the nonlinear creep model is closer to the actual failure characteristics of a layered soft rock tunnel through the verification of actual engineering simulation. The research results have certain theoretical design and project guiding significance for layered soft rock tunnel engineering.

2 Rock Mechanics Test

2.1 Test results of conventional mechanical characteristics test

To obtain the related parameters such as cohesion c, internal friction angle $\varphi$and elastic modulus$E$of layered soft rock, the conventional uniaxial-triaxial compression test was carried out on the rock. The test object was layered soft rock, a total of 18 samples, 3 samples in each uniaxial group and 5 samples in each triaxial test group. The compressive stress-strain curves of layered soft rock are shown in Figure 1, where the confining pressures of the triaxial compression test are 3 MPa, 6 MPa, and 9 MPa, respectively.

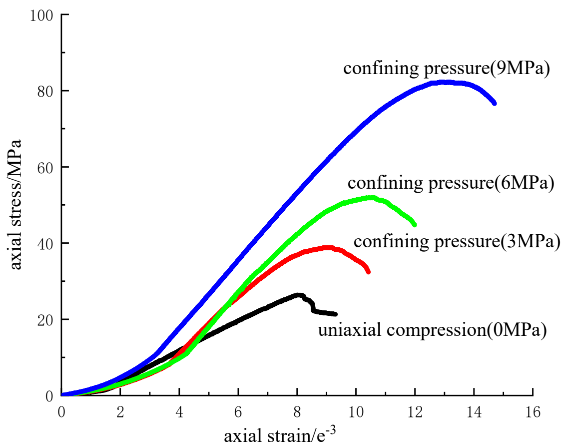

Fig. 1. Compression stress-strain curve of typical layered soft rock

It is observed from the above rock compression stress-strain curve that the rock deformation includes four stages: compaction stage, linear elastic stage, plastic failure stage, and brittle failure stage. Rock is a heterogeneous body with cracks, pores, and bedding defects. When the axial pressure was applied, the internal defects of the rock were compacted. With the increase of axial stress, the void ratio in the sample decreased, and the stress-strain curve showed an upward trend. With the increase of axial stress, the rock showed relatively obvious linear elasticity. With the further increase of axial stress, the number of rock fractures increases gradually, and many fractures are connected. Shear failure occurs along a certain structural plane, and the rock enters the stage of unstable expansion. After reaching the peak strength, the rock is destroyed, and the rock still has a certain strength after destruction. According to the uniaxial compression test, uniaxial compressive strengthσ_c, triaxial compressive strength σ_s, elastic modulus E and Poisson' ratio μ of rock are obtained. Then according to the Mohr-Coulomb strength criterion, rock cohesion c and internal friction angle φ are obtained. The specific test results are shown in Table 1.

Table 1. Conventional mechanical parameters of layered soft rock

σ_3/MPa	$\sigma_c(\sigma_s)$/MPa	E/GPa	μ	c/MPa	φ/°
0	26.95	4.53	0.26		
3	38.85	6.49	0.25	4.30	46.51
6	51.84	7.42	0.24		
9	82.30	8.24	0.23		

2.2 Test results of creep characteristics

According to the compressive strength of the rock in Table 1, the axial load of the uniaxial creep test is divided into 4 grades. The load of each grade is 70% ~ 85% of the corresponding axial pressure, and the loading pressure of each grade is 18.87 MPa, 20.21 MPa, 21.56 MPa, and 22.90 MPa respectively. The creep test lasted for about 12 h at all levels, but it did not include the accelerated creep stage. The accelerated creep stage was short, and the loading time was 36.38 h. The data were processed by the Boltzmann superposition principle. The overall loading curve and graded loading curve of rock under uniaxial and different confining pressures were obtained as shown in Figures 2- 5, where T was the loading time and ε was the axial strain.

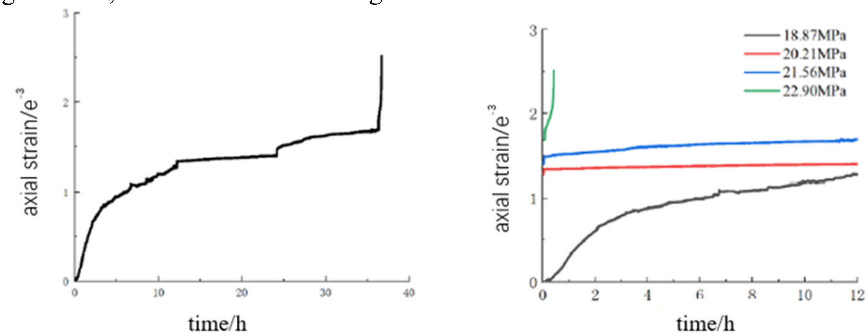

(a) overall loading curve (b) graded loading curve

Fig. 2. Overall creep loading curve

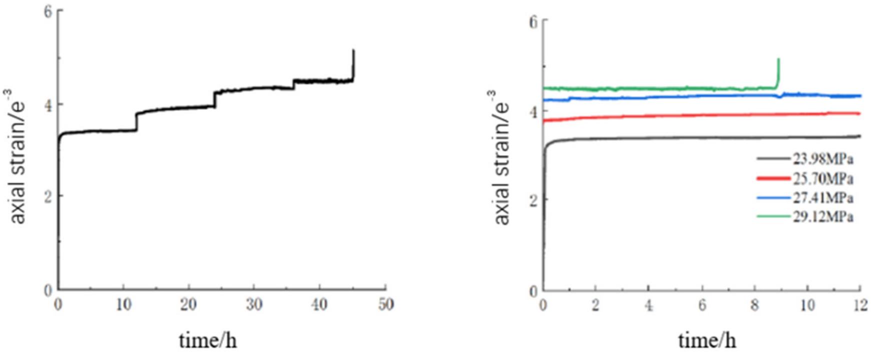

(a) overall loading curve (b) graded loading curve

Fig. 3. Creep curve of layered soft rock under 3 MPa confining pressure

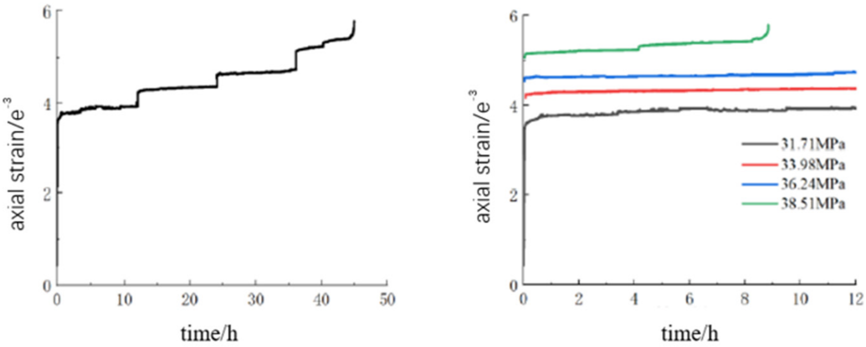

(a) overall loading curve (b) graded loading curve

Fig. 4. Creep curve of layered soft rock under 6 MPa confining pressure

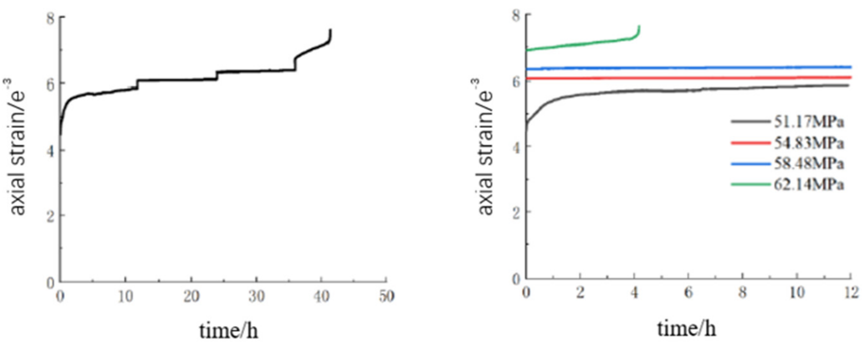

(a) overall loading curve (b) graded loading curve

Fig. 5. Creep curve of layered soft rock under 9 MPa confining pressure

3 Creep model improvement and parameter identification

The linear Burgers creep model has a poor effect in describing the accelerated creep stage of rock. In this paper, a plastic element is introduced based on the Mohr-Coulomb criterion, and a new improved Burgers nonlinear creep model is formed in series with the Burgers model. The visco-elastoplastic and elastoplastic properties are used to describe the partial stress and volume deformation of rock, respectively.

Through the above theoretical calculation, the creep parameters of layered soft rock can be obtained, and the Burgers-Mohr nonlinear creep simulation is used to fit the test parameters by Origin software. The overall fitting curve and the fourth-stage loading fitting curve are shown only, and compared with the linear Burgers fitting curve. The experimental data and fitting curves are shown in Figures 6-9.

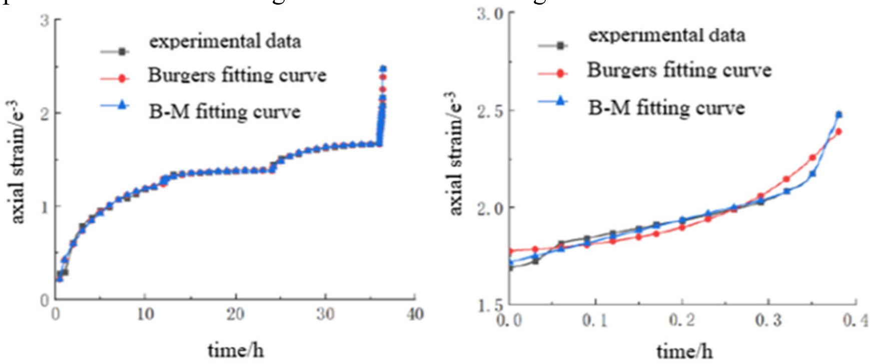

(a) overall fitting curve (b) fourth-order loading fitting curve

Fig. 6. The fitting curve of the uniaxial compression creep test

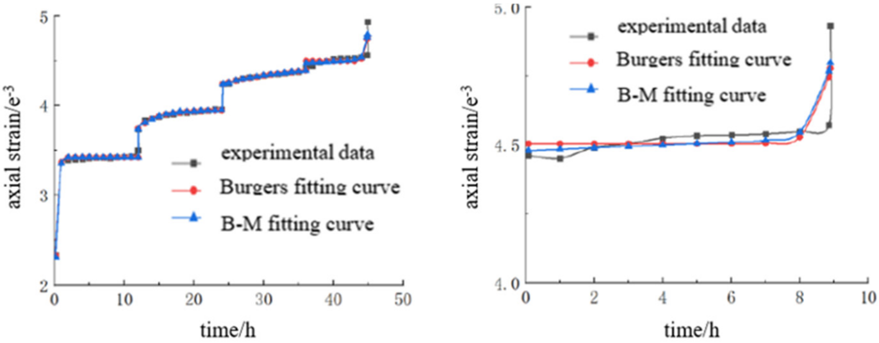

(a) overall fitting curve (b) fourth-order loading fitting curve

Fig. 7. The fitting curve of the 3 MPa compression creep test

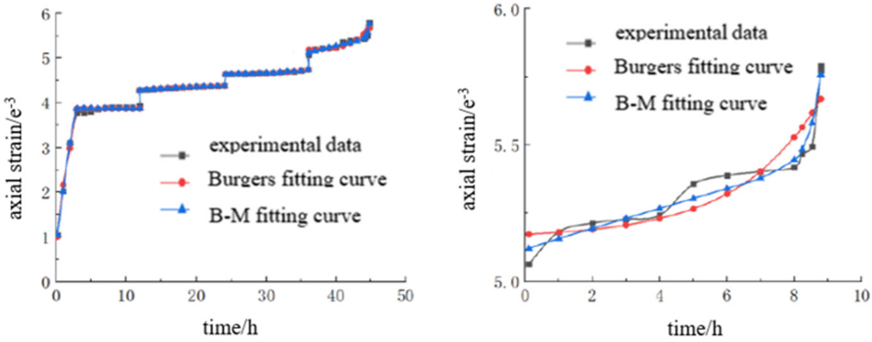

(a) overall fitting curve (b) fourth-order loading fitting curve

Fig. 8. The fitting curve of the 6 MPa compression creep test

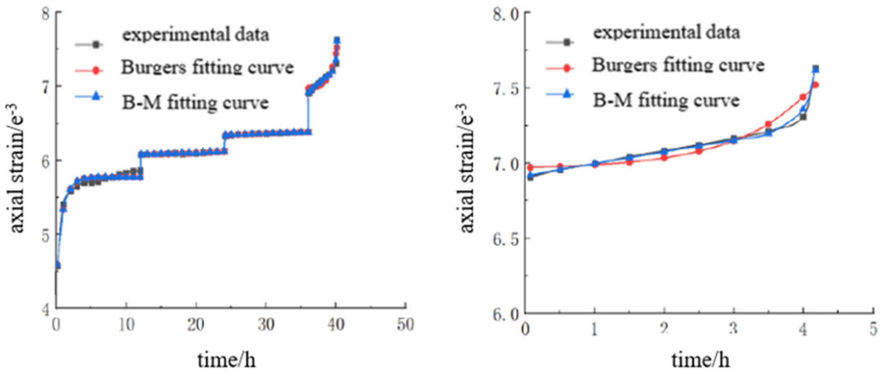

(a) overall fitting curve (b) fourth-order loading fitting curve

Fig. 9. The fitting curve of the 9 MPa compression creep test

From the fitting results, the fitting degree of the nonlinear Burgers-Mohr creep model is significantly higher than that of the linear Burgers creep model. Under the fourth stage of loading, the fitting R^2 of confining pressure 0 MPa, 3 MPa, 6 MPa, and 9 MPa are 0.9921, 0.9477, 0.9640, and 0.9916, respectively. Compared with the linear Burgers creep model, the fitting degree of the fourth stage of creep under different confining pressures increases by 7.53 %, 2.16 %, 9.30 %, and 10.82 %, respectively, which satisfies the fitting degree of 0.95, indicating that the improved model can more accurately describe the accelerated creep stage of layered rock mass and is closer to the creep condition of this kind of rock. The Burgers-Mohr nonlinear creep model can be applied to the creep analysis of layered soft rock in the tunnel.

4 Model application and verification

4.1 Model establishment

This simulation takes a layered soft rock tunnel as the research object. At the entrance and exit of the tunnel, there is a layered soft rock with mudstone and sandstone. To verify the reliability of the model parameters, numerical simulation is carried out based on the actual project. The model is 100 m × 100 m × 100 m cube and the tunnel depth is 70 m. The numerical simulation parameters and creep model parameters of the layered soft rock tunnel are shown in Table 2.

Table 2. Numerical simulation parameters of layered soft rock

Rock formation	Elastic modulus E/gpa	Cohesion C/kpa	The angle of internal friction *Φ*/°	Density *P/g/cm3*	Poisson ratio *M*
Layered rock	6.51	3.39	34.35	2450	0.20
Medium weathered sandstone	7.14	8.92	32	2430	0.22
Weakly weathered sandstone	8.68	8.25	34	2500	0.24
Anchor/steel frame	210	-	-	7800	0.30
C25 concrete	28	-	-	2550	0.20

4.2 Spatial Effect of Surrounding Rock in Layered Soft Rock Tunnel Construction

This simulation takes 3 m as excavation footage, which is divided into 34 construction stages, i.e., 34 days. It is assumed that the excavation speed is not affected by external factors, and 3 m is excavated stably every day. The Mohr-Coulomb constitutive model is used to simulate the tunnel excavation without considering the time effect, and the improved nonlinear Burgers - Mohr constitutive model is used to simulate the tunnel excavation considering the time effect.

Taking the tunnel section DK803 + 020 as an example, without considering the time effect, the stress-strain nephogram of tunnel excavation is shown in Figure 10.

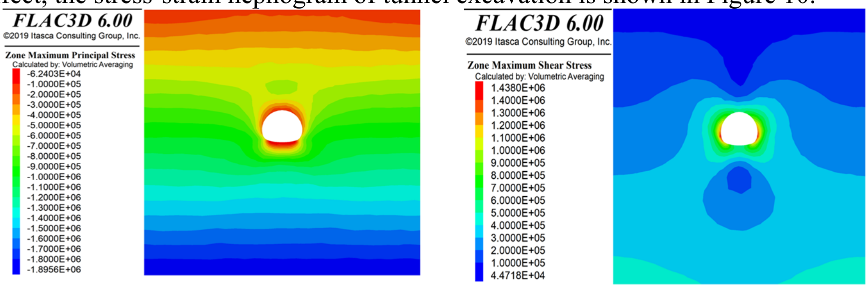

(a) maximum principal stress nephogram (b) maximum shear stress nephogram

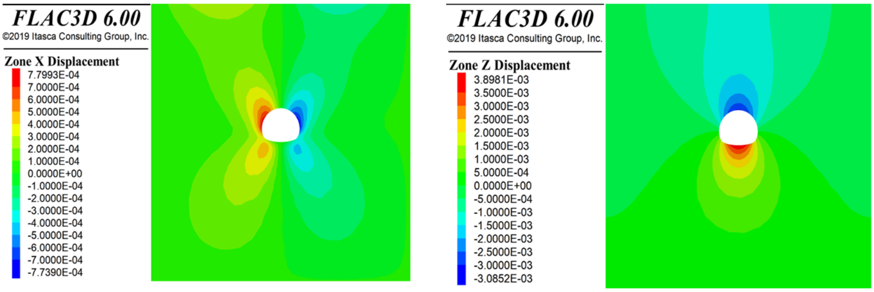

(c) cloud image of lateral displacement (d) vertical displacement nephogram

Fig. 10. Stress-strain nephogram without considering time effect

It can be seen from the stress nephogram that the stress concentration after tunnel excavation is distributed at the arch foot of the tunnel. The maximum principal stress is about 1.10 MPa, which is located at the arch foot of the tunnel. The minimum principal stress is about 3.24 MPa, which is distributed from the arch waist to the arch foot. The maximum shear stress appears at the arch waist, which is about 1.44 MPa. The stress monitoring curve of the arch foot is shown in Figure 11. It can be seen from the displacement nephogram that the lateral displacement is distributed at the arch waist, and the vertical displacement is distributed at the vault and bottom of the tunnel. The displacement changes of the left line and the right line of the tunnel are symmetrical, and the maximum values of the left line displacement and the right line displacement are about 7.80 m and 7.74 m, respectively. The maximum vault settlement is about 3.08 mm, and the maximum arch bottom uplift is about 3.90 mm. Monitoring curves of the vault, waist, and bottom displacements are shown in Figure 12.

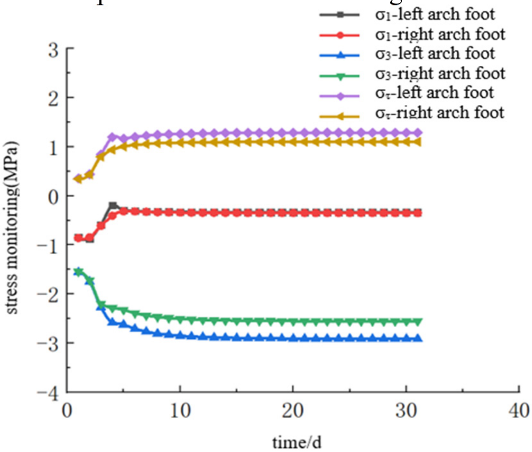

Fig. 11. Stress monitoring curve of arch foot

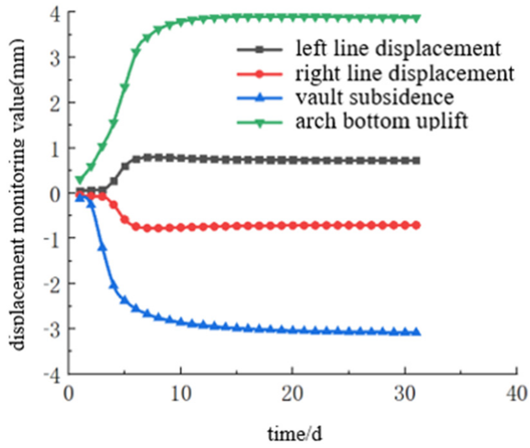

Fig. 12. Displacement monitoring curve

4.3 Spatial effect of surrounding rock in layered soft rock tunnel construction considering time effect

The improved nonlinear Burgers-Mohr model is used to simulate the tunnel construction process, and the stress-strain nephogram after excavation is shown in Figure 13. The stress monitoring curve is shown in Figure 14, and the displacement monitoring curve is shown in Figure 15.

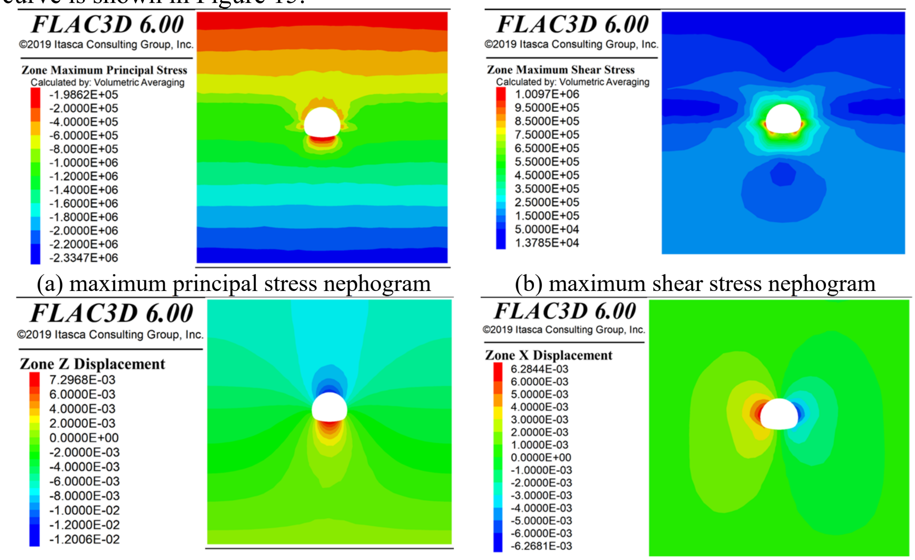

(a) maximum principal stress nephogram (b) maximum shear stress nephogram

(c) cloud image of lateral displacement (d) vertical displacement nephogram

Fig. 13. Stress nephogram of tunnel construction

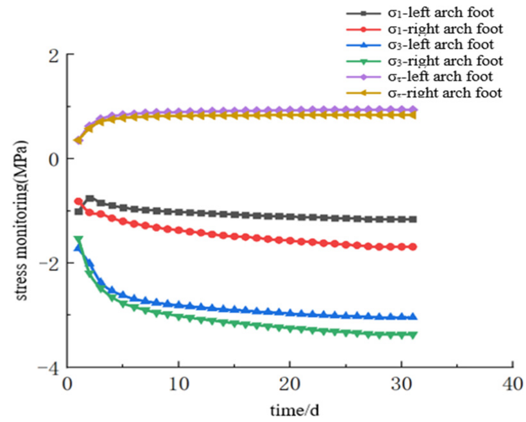

Fig. 14. Stress monitoring curve of arch foot

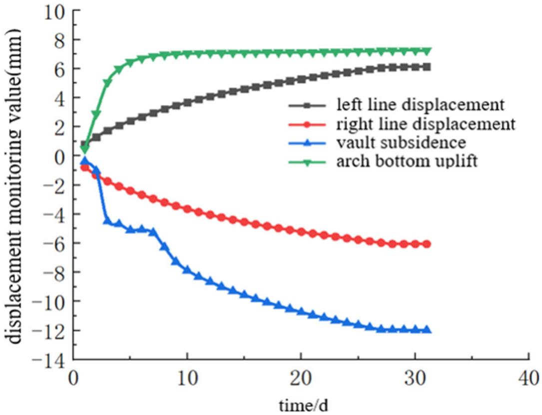

Fig. 15. Displacement monitoring curve

From the stress nephogram, the stress is symmetrically distributed along the tunnel axis. Different from the mechanical characteristics of surrounding rock without considering the time effect, the maximum principal stress and minimum principal stress are located at the arch foot, which are 1.50 MPa and 3.12 MPa respectively. The maximum shear stress is about 1.00 MPa, located at the tunnel arch waist. Through the displacement analysis, under the condition of considering the time effect, the maximum displacement of the left line is about 6.28 mm, and the maximum displacement of the right line is about 6.27 mm. The deformation of the left and right lines of tunnel excavation is symmetrical, the maximum settlement of the vault is about 12.00 mm, and the maximum uplift of the arch bottom is about 7.30 mm.

5 Conclusions

(1) The basic mechanical parameters and uniaxial-triaxial compression creep curves of layered soft rock are obtained by mechanical properties test. The results show that the compressive strength and elastic modulus of rock increase with the increase of confining pressure, and Poisson's ratio tends to be stable. Based on the Mohr-Coulomb strength criterion, the rock cohesion c is 4.30 MPa, and the internal friction angle φ is 46.51°. The creep characteristic curve includes the attenuation creep stage, stable creep stage, and accelerated creep stage.

(2) The linear Burgers creep model was used to fit the test data, and the fitting effect in the accelerated creep stage was poor. Based on the Mohr-Coulomb criterion, a plastic element is introduced and connected with the Burgers model in series to form a new improved Burgers nonlinear creep model. The improved model is used to fit the test data, and the fitting R^2 of the creep stage is significantly increased from 0.9226 to 0.9921, which shows that the nonlinear model can describe the accelerated creep stage of layered soft rock more accurately than the linear model.

(3) The code of improved nonlinear Burger's creep model is written based on $FLAC^{3D}$ embedded FISH language. The numerical simulation of the tunnel excavation stage is carried out by using the parameters of data fitting. The results show that the deformation law of the creep model tunnel is like the actual deformation law and the numerical value of the project, indicating that the model can well reflect the creep characteristics of the surrounding rock of the layered soft rock tunnel. It provides some theoretical and technical guidance for the construction design and mechanical analysis of similar layered soft rock tunnels.

Acknowledgments

Chongqing University of Science and Technology Students Innovation Training Program (202211551009, 2022136); Chongqing University of Science and Technology Research Fund Project (CK181901004).

References

1. Bustamante, R., S. Montero & A. Ortiz-Bernardin (2020) A novel nonlinear constitutive model for rock: Numerical assessment and benchmarking. *Applications in Engineering Science,* 3.
2. Gao, Y., F. Gao & Y. Manchu Ronald (2013) Rock creep modeling based on discontinuous deformation analysis. *International Journal of Mining Science and Technology,* 23**,** 757-761.
3. Gutiérrez-Ch, J. G., S. Senent, P. Zeng & R. Jimenez (2022) DEM simulation of rock creep in tunnels using Rate Process Theory. *Computers and Geotechnics,* 142.
4. Khalymendyk, I. & A. Baryshnikov (2018) The mechanism of roadway deformation in conditions of laminated rocks. *Journal of Sustainable Mining,* 17**,** 41-47.

5. Li, C., J. Wang & H. Xie (2020) Anisotropic creep characteristics and mechanism of shale under elevated deviatoric stress. *Journal of Petroleum Science and Engineering,* 185.
6. Man, J., H. Huang, Z. Ai & J. Chen (2022) Analytical model for tunnel face stability in longitudinally inclined layered rock masses with a weak interlayer. *Computers and Geotechnics,* 143.
7. Montero-Cubillo, N. S., R. A. Galindo, C. Olalla & M. Muñiz-Menéndez (2021) Pull-out creep laboratory test for soft rocks. International Journal of Rock Mechanics and Mining Sciences, 144.
8. Zha, E., Z. Zhang, R. Zhang, S. Wu, C. Li, L. Ren, M. Gao & J. Zhou (2021) Long-term mechanical and acoustic emission characteristics of creep in deeply buried Jinping marble considering excavation disturbance. International Journal of Rock Mechanics and Mining Sciences, 139.
9. Zhang, P., S. Ren, Y. Zhao, L. Wang, N. Long, F. Chen & C. Liu (2021) Combined effects of sulfate attack under drying–wetting cycles and loading on the fatigue behavior of concrete. *Advances in Structural Engineering,* 24**,** 3825-3836.
10. Wei, Y., Q. Chen, H. Huang & X. Xue (2021) Study on creep models and parameter inversion of columnar jointed basalt rock masses. *Engineering Geology,* 290.